Front. Phys., 2012, 7(6): 708–713
DOI 10.1007/s11467-012-0262-z

RESEARCH ARTICLE

Major elements analysis in bituminous coals under different ambient gases by laser-induced breakdown spectroscopy with PLS modeling

Zhe Wang, Ting-Bi Yuan, Siu-Lung Lui, Zong-Yu Hou, Xiong-Wei Li, Zheng Li†, Wei-Dou Ni

State Key Lab of Power Systems, Department of Thermal Engineering, Tsinghua-BP Clean Energy Center, Tsinghua University, Beijing 100084, China

E-mail: †lz-dte@tsinghua.edu.cn

Received February 24, 2012; accepted July 23, 2012

Three major elements, carbon, hydrogen, and nitrogen, in twenty-four bituminous coal samples, were measured by laser-induced breakdown spectroscopy. Argon and helium were applied as ambient gas to enhance the signals and eliminate the interference of nitrogen from surrounding air. The relative standard deviation of the related emission lines and the performance in the partial least squares (PLS) modeling were compared for different ambient environments. The results showed that argon not only improved the intensity, but also reduced signal fluctuation. The PLS model also had the optimal performance in multi-element analysis using argon as ambient gas. The root mean square error of prediction of carbon concentration decreased from 4.25% in air to 3.49% in argon, while the average relative error reduced from 4.96% to 2.98%. Hydrogen line demonstrated similar improvement. Yet, the nitrogen lines were too weak to be detected even in an argon environment which suggested the nitrogen signal measured in air come from the breakdown of nitrogen molecules in the atmosphere.

Keywords laser-induced breakdown spectroscopy (LIBS), ambient gas, bituminous coal, partial least squares (PLS), relative standard deviations (RSD)

PACS numbers 06.20.fb, 42.62.Eh, 52.25.Kn, 42.62.Fi

1 Introduction

Coal is one of the most important primary energy sources, especially in China. An accurate analysis of coal composition is very useful to improve the combustion efficiency and reduce pollutants and CO_2 emission. In China, since the thermal power plants periodically change the source of coal or use blending coal [1, 2], the industry always looks for a suitable method for fast or *in situ* assess of coal quality. The multi-element analysis technique, laser-induced breakdown spectroscopy (LIBS), is a promising solution for this application because of its real-time analysis capability, ease of implementation, and minimal sample preparation.

Coal is also one of the materials which cannot be easily studied by most spectroscopic techniques, including LIBS. It possesses a severe matrix effect due to its complex composition and structure. Line interference also prevents accurate analysis. Nevertheless, a significant amount of work of metal analysis in coal samples by LIBS has been conducted [2–7]. Ctvrtnickova *et al.* performed a series of studies to measure different elements in the fly ash of coal with LIBS [2–4]. Gaft *et al.* also demonstrated the online monitoring of metal content of coal ashes [5]. Yet, there are only a few reports of LIBS studies on the major non-metal compositions like carbon, hydrogen, and nitrogen [6, 7]. This is because these elements usually have fewer characteristic lines and their intensities were weak. Most importantly, the atmospheric condition has two negative impacts on the analysis. Firstly, some of these elements can be easily depleted by forming oxides in the atmosphere. Secondly, nitrogen from the ambient air can adversely affect the concentration prediction accuracy in nitrogen assay.

In most reported LIBS studies on coal samples, the measurements are usually performed on ash which is produced after the coal combustion [3–5]. To the best

of our knowledge, simultaneous quantitative analysis of C, H, and N of coal samples with LIBS has not been reported. LIBS analysis of these elements is better performed under an inert gas environment, where the influence of the nitrogen and oxygen in the atmosphere is minimized. The effects of ambient gas on LIBS have been comprehensively studied by the LIBS community [8–10]. A clear picture has been established for the influences of gas type and pressure on the plasma temperature and electron density. Bogaerts *et al.* revealed that a heavier background gas can slow down the plasma expansion. Heat loss through free expansion and particle collisions was reduced so the plasma can stay longer at its optimum emission temperature [8]. Ma *et al.* studied the temporal and spatial dynamics of a laser-induced aluminum plasma in an argon background, confirmed that the homogeneity and stability were improved [11]. Li *et al.* demonstrated that the LIBS emission of a coal sample was enhanced under an argon environment [12]. Despite these findings, not much is known about the ambient environment effects on the signal fluctuation and measurement accuracy.

In this paper, the major elements, C, H, and N in bituminous coals are studied by LIBS to evaluate the signal stability and prediction accuracy under atmospheric, helium, and argon environments. The LIBS setup and the experimental parameters are introduced in the next section. Then, the relative standard deviations (RSD) of the signals under different environments are compared, and the spectra are analyzed by the partial least squares (PLS) algorithm. The prediction results are evaluated for the applicability of LIBS on real-time bituminous coal analysis.

2 Experimental setup

The same Spectrolaser 4000 system (XRF Scientific, Australia) described in our previous paper was used in this study [13]. Briefly, a Nd:YAG laser (532 nm, 7 ns, 1 Hz) fired a laser pulse which was focused by a converging lens of 5 cm focal length onto the sample. The plasma emission was collected to a detection system equipped with four Czerny-Turner spectrographs and CCD detectors. The spectral bandwidth was from 190 nm to 940 nm, with a resolution of 0.09 nm.

Twenty-four bituminous coal samples were analyzed. The samples were in the form of powder, and were pressed into pellets (ϕ = 30 mm, h = 3 mm) with a hydraulic jack under a pressure of 20 tons [6]. Table 1 lists the concentration of C, H, and N of the samples which were certified by the China Coal Research Institute (CCRI). The pellets were mounted inside a chamber that was flushed by different inert gases at a flow rate of 2 L/min. The gas had a purity of 99.99%. The gas inlet and outlet were installed close to the pellet. Before capturing a spectrum, the chamber was flushed with the gas for 30 minutes to ensure the purity of the chamber.

Table 1 Major composition of bituminous samples.

		C/%	H/%	N/%
Calibration set	1	81.45	3.52	1.34
	2	78.98	4.95	1.38
	3	79.80	3.80	1.10
	4	67.28	3.68	1.05
	5	58.12	3.40	1.06
	6	54.21	2.53	0.74
	7	72.94	4.46	1.29
	8	79.22	3.28	1.07
	9	75.96	4.52	1.33
	10	76.69	4.42	1.08
	11	77.28	4.42	1.21
	12	78.58	4.59	1.32
	13	52.61	3.45	1.00
	14	53.42	3.50	0.97
	15	59.91	3.90	1.11
	16	67.77	4.25	1.20
	17	55.67	3.22	1.02
Validation set	18	81.54	3.70	1.16
	19	47.12	2.48	0.73
	20	55.14	2.79	0.84
	21	60.03	3.73	1.04
	22	78.78	5.01	1.31
	23	74.70	4.47	1.02
	24	70.45	3.40	1.15

Seventeen samples were selected for calibration of the PLS model while the rest were for validation. In order to test the robustness of the PLS model, the validation samples were chosen so that some of their elements had their concentrations fall outside the calibration ranges. For instance, sample 19 of the prediction set had a C concentration of 47%, while the lowest in the calibration set was 52%. The software used for the PLS calculation was Unscrambler 10.0 (CAMO, Woodbridge, NJ, USA).

In the experiment, two shots were fired at each of the 40 positions on a pellet. The first shot at 150 mJ was for cleaning and the second shot at 120 mJ was for analysis. The gate delay and exposure time were 2 μs and 1 ms, respectively. The intensity was defined as the integrated line area above the background continuum. All spectra were background subtracted and then normalized with the segmental spectral area [6].

As mentioned previously, there were only a few emission lines for the interested elements. With our LIBS system operating under atmospheric condition, carbon had two visible and well-defined lines at 193.09 nm and 247.86 nm. Hydrogen line was observable at 656.28 nm. Nitrogen showed a weak triplet at 742.36, 744.29, and 746.83 nm. Nevertheless, the lack of emission lines for these elements make the statistics based PLS method

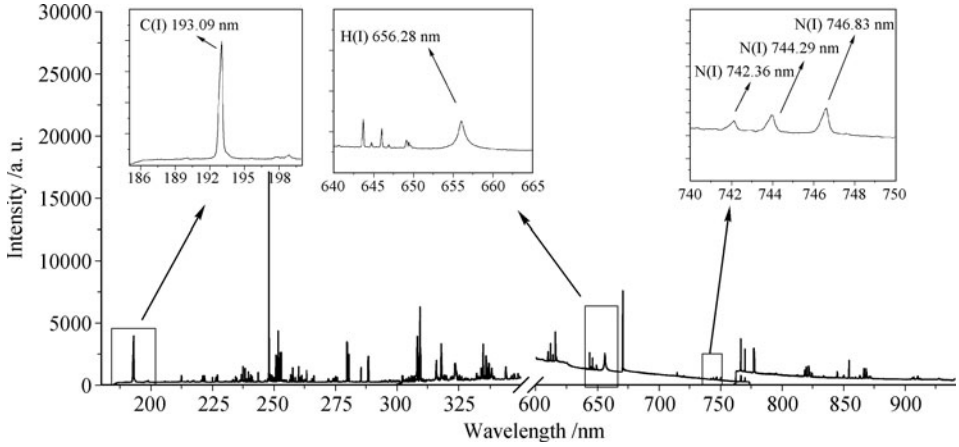

Fig. 1 A typical LIBS spectrum of Coal Sample 1 measured in air.

preferable in constructing the calibration model. A typical coal sample spectrum under air was shown in Fig. 1.

3 Results and discussion

3.1 Plasma characteristics

The strength of the plasma emission depends on the properties of the surrounding ambient gas [11, 14]. Table 2 lists the physical properties of the gases in this study. Before focusing on the study objective, the effect of the ambience to the plasma is inspected and compared with previous reports. Two parameters, plasma temperature (T) and electron number density (n_e), are often used to describe a LIBS plasma. In our study, the temperature is obtained from the Boltzmann plots of the aluminum lines, while the electron density is calculated from the Stark width of the hydrogen 656.28 nm line by Ref. [15] using

$$n_e = C(n_e, T)\Delta\lambda_s^{3/2} \quad (1)$$

where $\Delta\lambda_s$ is the half width of broadened line and $C(n_e, T)$ is a weak function of n_e and T which can be found in Ref. [15].

The plasma temperature and electron densities for each calibration samples in different ambient gases are calculated and plotted in Fig. 2. The error bars in Fig. 2 indicate the standard deviation of the 40 shots on each sample. As shown in Fig. 2(a), plasma temperatures for the case of helium and argon are higher than that of air. The higher temperature in an argon environment can be attributed to its relatively lower thermal conductivity that helps to preserve the heat of the plasma. On the other hand, the higher temperature in a helium environment is due to the considerably higher ionization energy of the gas, so more energy is deposited onto the plasma.

Conversely, the electron density is the highest in air and the lowest in a helium environment. Helium is the lightest among the three gases, so its confinement strength is the weakest. The plasma expands fast and the density drops. For argon and air, they are much heavier so they have better caging effect. For air, extra electrons

Table 2 The physical properties of different ambient gases.

Parameters	Air	He	Ar
Specific heat capacity /(J·g^{-1}·K^{-1})	1.00	5.23	0.54
Thermal conductivity /(10^{4}W·cm^{-1}·K^{-1})	2.60	15.1	1.77
Ionization energy/(kJ·mol^{-1})	N_2: 1402.3 O_2: 1313.9	2372.3	1520.6
Atomic weight	N_2: 28 O_2: 32	4	40

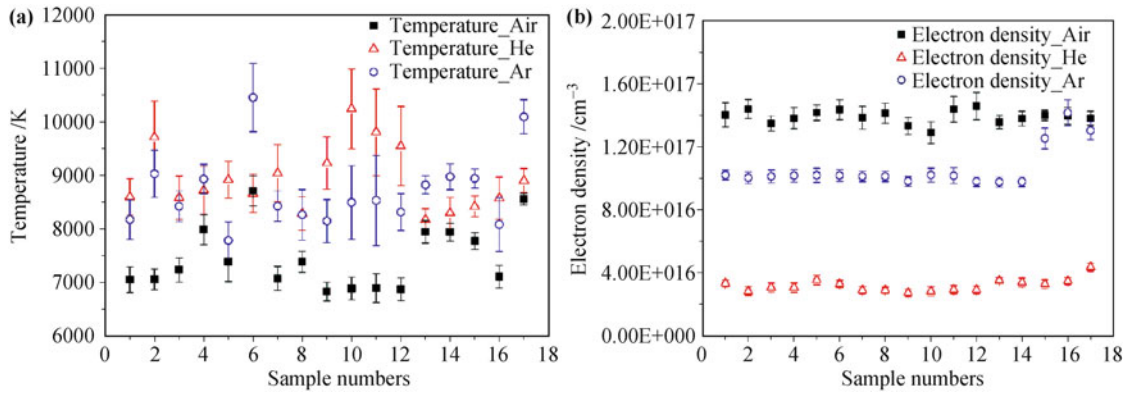

Fig. 2 The plasma temperature and electron density of 17 samples in the calibration set.

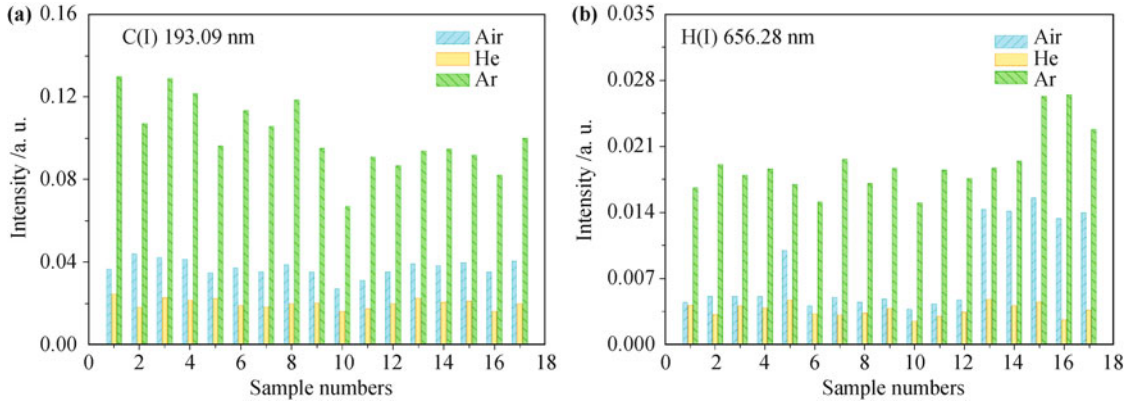

Fig. 3 Comparison of the intensities of different lines in various ambient gases for the calibration samples: **(a)** C(I) 193.09 nm, **(b)** H(I) 656.28 nm.

are generated from the nitrogen and oxygen breakdowns so the electron density is the highest [11, 14]. Overall, the characteristic of plasma temperature and electron density of the coal plasma are similar to those in other publications. Most of the observations and findings reported about the ambient effects on LIBS can thus be applied to coal samples. In addition, the McWhirter criterion was used in validating the local thermodynamic equilibrium (LTE) condition [16]. The electron densities meet the minimum requirement of 10^{16} cm^{-3}. The other two criteria of LTE were also used for LTE assessment based on Ref. [17]. The relaxation time of C(I) 193.09 nm and H(I) 656.28 nm are in the order of 10^{-6} s and 10^{-10} s, respectively. They are much shorter than the time scale of the plasma expansion. Similarly, the diffusion length during the relaxation time of the analytical lines were about 10^{-5} m for C(I) 193.09 nm line and 10^{-8} m for H(I) 656.28 nm line, which were much smaller than the plasma diameter 10^{-3} meter. Consequently, the assumption of LTE could be fulfilled in the present work. The next section continues with the evaluation of the signal stability which has not been previously investigated.

3.2 Line intensity

The line intensities of different lines, C(I) 193.09 nm, H(I) 656.28 nm, and N(I) 746.83 nm are examined under three ambient gas environments (Fig. 3). The enhancements in different ambient environments vary with the lines. For carbon and hydrogen lines, a twofold to threefold signal boost is recorded in the argon environment. This observation is consistent with the findings by Harilal et al. [18]. The intensity of N lines at 742.36, 744.29, and 746.83 nm in three ambient gas environments were examined in Fig. 4. The three lines were only visible in air. However, in carbon and hydrogen analysis, it is the argon environment that has the best signal enhancement. This suggests the nitrogen signal recorded in the air experiment is probably originated from the breakdown of N_2 in air. Therefore, in order to accurately measure the nitrogen concentration in coal samples, an environment other than air must be used.

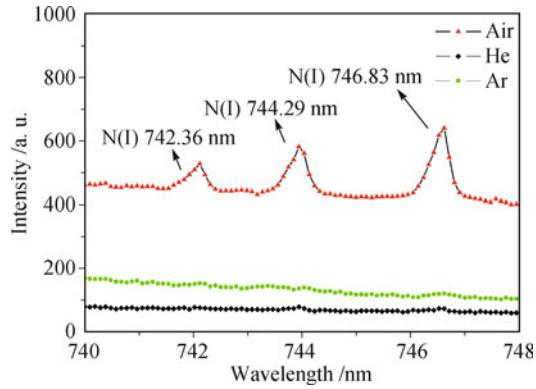

Fig. 4 Comparison of the intensities of nitrogen lines of Sample 1 in various ambient gases.

3.3 RSD comparison

The intensities of the lines are normalized by the corresponding segmental spectral area before their RSD are compared [6]. Table lists the average RSD of the line intensities of all samples for the three ambient gas environments. Signals measured in an argon environment have the lowest RSD in the case of C and H. This indicates that the emissions are more stable. Under an argon environment, the LIBS plasma is better confined and the heat loss is minimal. This provides a favorable condition for the plasma emission. For nitrogen, the RSD in the air experiment is not analyzed as the signals are not from the nitrogen in coal samples. In argon and helium, the nitrogen lines are barely visible, so the RSD are also not available.

In a helium environment, the RSD are always the worst because of the poor caging effect. In short, under an argon environment, the signal enhancement is always accompanied by improved signal stability. Its effect on the accuracy of PLS modeling is discussed next.

3.4 PLS modeling comparison

PLS modeling is one of the popular chemometric tools for quantitative analysis of LIBS in the past decade [19–

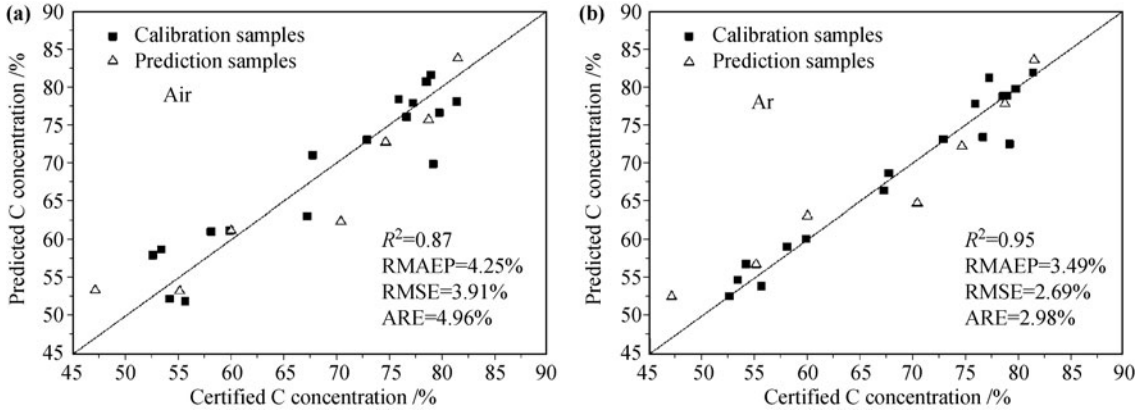

Fig. 5 Comparison of the calibration and prediction results of carbon concentration in atmospheric **(a)** and argon **(b)** environments by PLS models.

Table 3 Comparison of the average RSD of line intensities of the calibration samples under three ambient gas conditions.

	C(I) 193.09 nm	H(I) 656.28 nm
Air	9.76%	6.75%
He	13.25%	9.84%
Ar	8.50%	6.19%

21]. A PLS model for predicting the concentration is established for different gases from the line intensities of the calibration set. The numbers of principal components (PC) are optimized based on the cross validation procedure. In this method, one random sample from the calibration set is selected as a temporary validation sample, while the rest are for establishing the model. When the PC number is optimized, a root mean square error of prediction (RMSEP) is obtained for the validation sample. These procedures are repeated for all calibration samples. Then, the optimum number of PC can be determined from the RMSEPs.

Since the carbon signal from the argon environment has the lowest RSD, the performance of the PLS model of carbon in argon is then compared to the one generated under the atmospheric condition. As observed from Fig. 5, the data points in an argon environment are less dispersed from the ideal line. The coefficient of determination R^2 is much higher at 0.95 when compared to that in air ($R^2 = 0.87$). Obviously, the least varying emission in an argon environment improves the robustness of the model. The RMSEP is reduced from 4.25% to 3.49%. The average relative error (ARE) also drops from 4.96% to 2.98%. In addition, the root mean square error (RMSE), which takes into account of both the calibration and prediction sets, is decreased from 3.91% to 2.69%. All enhanced accuracies indicate an improved model. Similar improvements of hydrogen data are also shown in Fig. 6. Clearly, the data set with a lower RSD has positive effects on the accuracy of the PLS model.

The performances of the PLS models are summarized in Table 4. The predictions show that noticeable RMSEP and RMSE improvement under an argon environment are attributed to the RSD enhancement. In addition, it should be noted that for the carbon and hydrogen concentration predictions in a helium environment, the RMSEP improves even though the RSD of the signals increase. A possible explanation is that, in a helium environment a plasma expands much faster and becomes less dense. The background continuum decreases, line broadening effect is reduced, and interferences between lines are diminished. Therefore, the emission lines are much clearer than those observed in air and argon environment. Despite the larger signal fluctuation in a helium environment, the improved accuracy of the line allow a

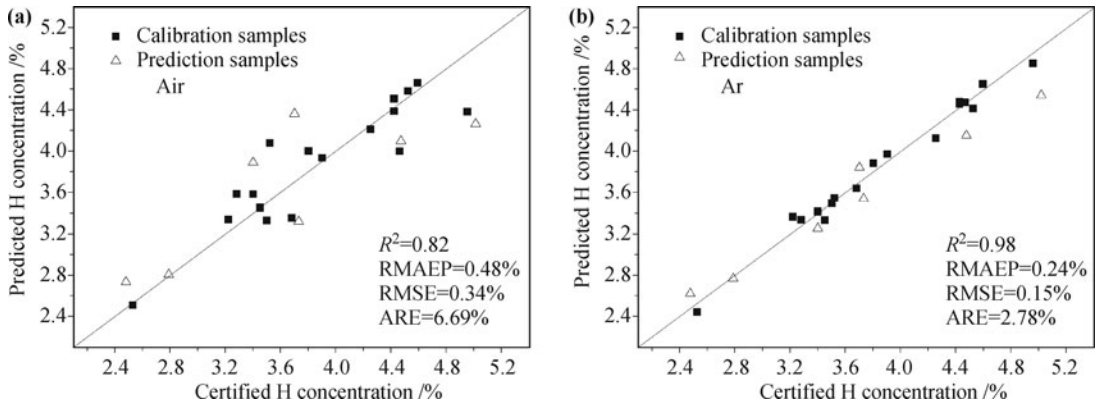

Fig. 6 Comparison of the calibration and prediction results of hydrogen concentration in atmospheric **(a)** and argon **(b)** environments by PLS models.

more precise PLS model to be established [22]. The differences between argon and helium to measurement uncertainty and accuracy indicate a two-faceted effect of plasma confinement. Further studies are required for optimizing the confinement effects in order to improve LIBS performance.

Table 4 Comparison of the performance of the PLS models of different gases.

	Ambiences	RSD/%	RMSEP/%	RMSE/%	R^2	ARE/%
C	Air	9.76	4.25	3.91	0.87	4.96
	He	13.25	3.32	2.43	0.96	2.81
	Ar	8.50	3.49	2.69	0.95	2.98
H	Air	6.75	0.48	0.34	0.82	6.69
	He	9.84	0.27	0.21	0.91	4.56
	Ar	6.19	0.24	0.15	0.98	2.78

4 Conclusions

In the present work, the concentrations of C, H, and N in 24 bituminous coal samples are measured by LIBS under atmospheric, helium, and argon environments. Plasma temperature and electron density are evaluated to ensure that LTE condition is fulfilled. Line enhancement of C and H are observed in an argon environment and the RSD of signals are reduced. The PLS model also demonstrates an improved accuracy owing to a higher quality for the spectra measured in the argon environment.

For the analysis of nitrogen, because of the seriously breakdown of N_2 in air, the analysis of nitrogen in coal must be done in an ambient gas environment. However, our results show that simply using ambience gas, such as argon or helium, is insufficient to enhance the weak nitrogen signal in coal samples. Other enhancement methods, like the application of a cavity confinement, the double-pulse technique, or other approaches [23–25], must be applied for signal improvement.

Practically, the conventional PLS method has some limitations. It only works best when the predicted concentration is within the calibration range. Outside the calibration limits, the prediction becomes inaccurate. It is also expected that, when the matrix of the sample significantly differs from those of the calibration set, the accuracy of the model declines. A revised model based on the dominant factor of the physical principles is proposed for multi-element measurement of the bituminous coal instead [26, 27]. Future work needs to focus on evaluating the performance of the revised models when they are applied to the inert gas environments.

Acknowledgements The authors are grateful for the financial support from the National Natural Science Foundation of China (Grant No. 51061130536).

References

1. M. Gaft, I. Sapir-Sofer, H. Modiano, and R. Stana, Spectrochim. Acta B, 2007, 62(12): 1496
2. T. Ctvrtnickova, M. P. Mateo, A. Yanez, and G. Nicolas, Appl. Surf. Sci., 2011, 257(12): 5447
3. T. Ctvrtnickova, M. P. Mateo, A. Yanez, and G. Nicolas, Spectrochim. Acta B, 2009, 64(10): 1093
4. T. Ctvrtnickova, M. P. Mateo, A. Yanez, and G. Nicolas, Spectrochim. Acta B, 2010, 65(8): 734
5. M. Gaft, E. Dvir, H. Modiano, and U. Schone, Spectrochim. Acta B, 2008, 63(10): 1177
6. J. Feng, Z. Wang, L. West, Z. Li, and W. D. Ni, Anal. Bioanal. Chem., 2011, 400(10): 3261
7. T. Yuan, Z. Wang, L. Li, Z. Hou, Z. Li, and W. D. Ni, Appl. Opt., 2012, 51(7): B22
8. A. Bogaerts, Z. Y. Chen, and D. Bleiner, J. Anal. At. Spectrom., 2006, 21(4): 384
9. Z. Y. Chen, D. Bleiner, and A. Bogaerts, J. Appl. Phys., 2006, 99(6): 063304
10. Effenberger and J. R. Scott, Anal. Bioanal. Chem., 2011, 400(10): 3217
11. Q. L. Ma, V. Motto-Ros, W. Q. Lei, M. Boueri, X. S. Bai, L. J. Zheng, H. P. Zeng, and J. Yu, Spectrochim. Acta B, 2010, 65(11): 896
12. J. Li, J. D. Lu, Z. X. Lin, S. S. Gong, C. L. Xie, L. Chang, L. F. Yang, and P. Y. Li, Opt. Laser Technol., 2009, 41(8): 907
13. J. Feng, Z. Wang, Z. Li, and W. D. Ni, Spectrochim. Acta B, 2010, 65(7): 549
14. G. Cristoforetti, G. Lorenzetti, S. Legnaioli, and V. Palleschi, Spectrochim. Acta B, 2010, 65(9—10): 787
15. H. R. Griem, Spectral Line Broadening by Plasmas, New York: Academic Press, 1974
16. A. W. Miziolek, V. Palleschi, and I. Schechter, Eds., Laser Induced Breakdown Spectroscopy (LIBS): Fundamentals and Applications, Cambridge: Cambridge University Press, 2006
17. G. Cristoforetti, A. De Giacomo, M. Dell'Aglio, S. Legnaioli, E. Tognoni, V. Palleschi, and N. Omenetto, Spectrochim. Acta B, 2010, 65(1): 86
18. S. S. Harilal, C. V. Bindhu, V. P. N. Nampoori, and C. P. G. Vallabhan, Appl. Phys. Lett., 1998, 72(2): 167
19. J. Amador-Hernandez, L. E. Garcia-Ayuso, J. M. Fernandez-Romero, and M. D. L. de Castro, J. Anal. At. Spectrom., 2000, 15(6): 587
20. S. C. Yao, J. D. Lu, J. Y. Li, K. Chen, J. Li, and M. R. Dong, J. Anal. At. Spectrom., 2010, 25(11): 1733
21. M. R. Dong, J. D. Lu, S. C. Yao, J. Li, J. Y. Li, Z. M. Zhong, and W. Y. Lu, J. Anal. At. Spectrom., 2011, 26(11): 2183
22. Y. Lida, Spectrochim. Acta B, 1990, 45(12): 1353
23. M. Gaft, L. Nagli, I. Fasaki, M. Kompitsas, and G. Wilsch, Spectrochim. Acta B, 2009, 64(10): 1098
24. W. D. Zhou, L. I. Kexue, Q. M. Shen, J. Shao, and H. G. Qian, Spectrochim. Acta B, 2010, 65(5): 420
25. W. D. Zhou, K. X. Li, X. F. Li, H. G. Qian, J. Shao, X. D. Fang, P. H. Xie, and W. Q. Liu, Opt. Lett, 2011, 36(15): 2961
26. Z. Wang, J. Feng, L. Z. Li, W. D. Ni, and Z. Li, J. Anal. At. Spectrom., 2011, 26(11): 2289
27. Z. Wang, J. Feng, L. Z. Li, W. D. Ni, and Z. Li, J. Anal. At. Spectrom., 2011, 26(11): 2175